Inelastic energy loss in low-energy Ne$^+$ scattering from a Si surface

F. Xu, G. Manicò, F. Ascione, A. Bonanno, and A. Oliva

Dipartimento di Fisica, Università della Calabria, 87036 Arcavacata di Rende, Cosenza, Italy

R. A. Baragiola

Department of Engineering Physics, University of Virginia, Charlottesville, Virginia 22903

We report a study on single scattering of 500–1950-eV Ne$^+$ ions from a Si surface. Our results show a sharp increase in the inelastic energy loss suffered by backscattered Ne$^+$ for the distance of closest approach R_{min} $\leqslant$0.59 Å. A detailed data analysis which considers both the continuous interactions with the target valence electrons and the discrete inelasticity Q_o in the binary Ne-Si collisions reveals a constant $Q_o = 45 \pm 4$ eV for $R_{min} \leqslant 0.47$ Å. This is attributed to the simultaneous excitation of two electrons from the neutralized Ne to the $2p^4(^1D)3s^2$ autoionization state. A small doubly charged Ne^{2+} single-scattering peak has also been observed for $R_{min} \leqslant 0.59$ Å. In this case, the inelasticity of 86 ± 5 eV in the binary collisions is ascribed to the two-electron excitation of surviving Ne$^+$ to Ne^{2+*} $2p^3 3s$. These assignments are consistent with all previously reported experimental results of autoionization electron emission, and the charge fraction, intensity, and energy spectral line shape of backscattered singly and doubly charged ions, for Ne$^+$ and Ne^0 impact on Si, Al, Mg, and Na surfaces. Our results indicate that in low-energy collisions the excited electrons can be located in bound atomic outer shells without being transferred to the conduction band of the solid. The similar threshold internuclear distances for the excitation of Ne $2p$ electrons for both Ne$^+$-Si and Ne^0-Si indicate that transitions occur at similar crossings of the promoted $4f\sigma$ molecular orbital (correlated to Ne $2p$) with high-lying empty orbitals. [S1050-2947(98)05801-6]

PACS number(s): 34.50.Dy, 34.50.Bw, 34.70.+e, 79.20.Rf

I. INTRODUCTION

Collision of low-energy ions with surfaces results in backscattering of the projectile and sputtering of target particles in various charge states, and emission of characteristic and secondary electrons and photons. Spectroscopic techniques based on the detection of these emitted particles can be used to study the surface structure and its elemental composition (for example, ion scattering spectroscopy; see Refs. [1,2] for reviews) and to investigate the details of the inelastic energy loss involved in atomic collisions in solids (e.g., spectroscopies of Auger or autoionization electrons and photons emitted from the projectile and target; see Refs. [3–5] for reviews). One of the most intriguing problems common to all techniques is the charge exchange between atomic species and surfaces [6,7]. Ever since the pioneering work of Hagstrum in the 1950s [8,9], resonant tunneling and Auger-type charge transfer mechanisms have been intensively studied both theoretically and experimentally [6,7,10]. However, it is only in recent years that the role played by core-electron excitation in determining the final charge state of scattered projectile has been explored [11–17].

Large ion fractions η^+ of backscattered He$^+$ and Ne$^+$ projectiles from a variety of elemental and compound surfaces were observed already some 20 years ago [18–25], and were generally attributed to the reionization in the violent collisions of projectiles neutralized on approach to the surface [26,27]. The same conclusion was drawn for the few measurements on the energy difference between the observed two peaks in the energy spectra of backscattered He$^+$ [23,25,28].

A very different scenario was described by Heiland and Taglauer, who measured the energy loss suffered by Ne$^+$ when reflected from Ag and Ni [29,30]. They proposed that the projectile Ne$^+$ ion is first neutralized to the ground state, then excited to an autoionization state, and finally decays into Ne$^+$. Grizzi *et al.* [12] correlated the large charge fraction for Ne$^+$ impact on Mg with the Ne $2p^4 3s^2$ autoionization electron emission and concluded that the high η^+ is due to the relatively large threshold internuclear distance for the formation of Ne**, and that the large decay distance from the surface where the probability for reneutralization is small. Very similar results and interpretations were given recently for Ne$^+$ scattering from other surfaces [14,15,31–33], and extended to the case of alkali projectiles [13,34].

Though there is a general consensus in attributing the high charge fraction in these systems to core-electron excitation in hard collisions, a detailed description of the excitation process is still being debated, especially regarding neon projectiles. The main issues concern the relative importance of one-electron versus simultaneous two-electron excitations in single binary collisions, the validity of the electron promotion model originally developed for gas-phase ion-atom collisions, and whether and how the band structure of the solid influences the electronic transition channels and probabilities [14, 35–40]. Previous studies were mainly based on the emission of autoionization electrons and photons, and charge fractions, and could provide little direct information on the excitation mechanism. The measurements of the inelastic energy loss of backscattered projectiles can solve this problem adequately, since it can directly determine the electronic transitions involved and discriminate whether these occur in single-, double-, or multiple-scattering events. However, precise and systematic inelastic energy-loss experi-

ments are quite difficult in most experimental conditions, and a careful and detailed data analysis procedure is required. In fact, in the early studies, the inelastic energy loss of the projectile was commonly used instead of the inelasticity, i.e., the center of mass or total (projectile and target) inelastic energy loss in the binary collision [20,23,28,31], and even in the most recent studies the continuous electronic stopping was still assumed to be independent of the particle charge state [32,33].

In this paper, we present a detailed investigation on the inelastic energy loss suffered by backscattered Ne$^+$ and Ne^{2+} ions for 500–1950-eV Ne$^+$ incident on a Si surface. Our study reveals that for small (500 eV) incidence energy, Ne$^+$ loses about 5–6 eV in the interactions with the surface, that its inelastic energy loss increases sharply once the distance of closest approach R_{min} reaches 0.59 Å, and that a constant inelasticity of 45 ± 4 eV occurs in the binary Ne-Si encounter when $R_{min} \lesssim 0.47$ Å. This energy loss is assigned to the Ne $2p^6 \rightarrow 2p^4(^1D)3s^2$ transition. For detected Ne^{2+} an inelasticity of 86 ± 5 eV was determined and is attributed to a double-electron excitation of a surviving Ne$^+$ into Ne^{2+*} $2p^3(^2D)3s$ or $2p^3(^2P)3s$. These results suggest that in the keV energy range two-electron excitation predominates over one-electron excitation and that the excited Ne $2p$ electrons are not necessarily transferred to the conduction band of the solid, but can be located in the bound atomic outer shells and, in this sense, the presence of the solid has little influence on the electronic transition channels and probabilities. The same threshold distance for excitation in Ne$^+$-Si and Ne^0-Si collisions suggest that transitions occur at the similar crossings of the promoted $4f\sigma$ (Ne $2p$) with high-lying empty levels. Our interpretation is consistent with all existing autoionization electron emission, charge fraction, and backscattering data in the literature for Ne incident on Si, Al, Mg, and Na surfaces.

II. EXPERIMENTAL PROCEDURE AND DATA ANALYSIS

A. Experimental procedure

The experiments were conducted in a UHV chamber with a base pressure of 5×10^{-10} Torr. Ne$^+$ ions were produced in a differentially pumped electron-impact-type ion source, and focused on the sample with an electrostatic lens. The discharge voltage was kept below the second ionization potential of Ne to avoid the eventual Ne^{2+} contamination. The beam divergence was less than 0.15°, as determined with a movable Faraday cup. The target was a single-crystal Si(111) wafer which was amorphized by prolonged ion bombardment. Sample cleaning was achieved by 2-keV Ne$^+$-ion sputtering, and verified with both Auger electron spectroscopy and Ne$^+$ ion scattering spectroscopy.

Backscattered Ne$^+$ and Ne^{2+} ions were analyzed with a rotatable hemispherical electrostatic energy analyzer placed in the incidence plane. The whole system was carefully aligned both optically and by directly measuring the incident beam. The analyzer has a total acceptance angle of 1.8°, and the precision in determining the scattering angle θ (relative to the beam direction) is better than 0.3°. In this study, all measurements were performed in specular reflection geometry (incidence angle relative to the surface $\alpha = \theta/2$). The analyzer was operated in a constant pass energy mode (20

eV) to ensure a constant detection efficiency of the channeltron multiplier, and the analyzer transmission function was carefully determined independently. The energy step between two consecutive data points was 0.5 eV. The doubly charged ions appeared in the spectra at half of their kinetic energies. The primary energies used in this study were 500, 700, 1000, 1400, and 1950 eV, which were measured directly at $\theta = 0°$. These energies were chosen to cover the whole range of closest approach distance R_{min} from 0.34 to 0.72 Å. The combined full width at half maximum of the energy spread of the ion beam and the resolution of the analyzer was about 2 eV.

B. Data analysis

Since the primary interest of this investigation is the inelastic energy loss suffered by the backscattered Ne$^+$ and Ne^{2+} ions in single scattering (SS) events, our data analysis and discussion will mainly focus on the behavior of the projectile inelastic energy loss $\Delta E = E_{elastic} - E_k$ as a function of θ. Here $E_{elastic}$ is the value predicted for elastic Ne-Si SS, and E_k is the measured kinetic energy. The distance of closest approach R_{min} reached in the collision is derived from θ by using the Thomas-Fermi-Moliére potential with a Firsov screening length a_u. We will also analyze the θ-dependent behavior of the linewidth Γ of the SS peaks, its intensity, and the ratio between the doubly and singly charged Ne.

To gain some quantitative information on the inelastic energy-loss mechanism, we consider the scattering process as composed of three distinct steps: (1) the incoming path, (2) the hard binary collision, and (3) the outgoing path. In steps (1) and (3) the projectile particle can undergo charge exchange with the surface and can be slowed down by exciting target electrons, whereas in step (2) discrete electronic transition may occur if the internuclear distance is sufficiently small [35,36]. This approach has been widely adopted in the literature [32,41,42], and can greatly facilitate our discussion on the inelastic energy loss mechanism.

We describe the continuous electronic slowing down in steps (1) and (3) by using the expression given by Oen and Robinson [43]:

$$Q_i = c_i \left(0.0274 \frac{\sqrt{E_i}}{\pi a_u^2} \right) \exp(-0.3 R_{min}/a_u), \qquad (1)$$

where E is the particle kinetic energy in eV, and the subindex $i = 1,3$ labels the incoming and outgoing paths, respectively. The constant c is a fitting parameter which is assumed to depend on the charge state of the particle ($c^0 < c^+ < c^{2+}$; see Ref. [44]). Since the typical distances for resonant or Auger neutralization and resonant reionization are larger than that of inelastic energy loss, the charge state we refer to is that of a Ne particle prior or subsequent to the binary collision.

We note that in the original work of Oen and Robinson [43], expression (1) was attributed to the total continuous inelastic loss, i.e., $Q_1 + Q_3$. A distinction between incoming and outgoing paths using the appropriate kinetic energies before and after the binary collision should be physically more meaningful, since here the essence is that the inelastic energy loss follows the spatial distribution of the electron

density which decays exponentially away from the target atom. The separation into two segments thus would result only in an apparent change of c. Though this model is essentially of atomic nature, it can be applied to ion scattering from surfaces with incidence and scattering angles which are not too small. Indeed, the great majority of the loss occurs within a very small distance from the target atom.

The projectile particle will collide with the target atom with an energy of $E_2 = E_1 - Q_1$ where $E_1 = E_p$ is the ion incidence energy. If we denote Q_{bin} as the total energy lost in the binary collision [step (2)] due to Ne-2p electron excitation, then the energy loss partitioned by the projectile, ΔE_{bin}, is given by

$$\Delta E_{bin} = E_2 \times \left\{ \frac{\mu}{(1+\mu)} \frac{Q_{bin}}{E_2} + \frac{2\cos\theta\sqrt{\mu^2-\sin^2\theta}}{(1+\mu)^2} \right.$$
$$\left. \times \left[1 - \left(1 - \frac{\mu(1+\mu)}{(\mu^2-\sin^2\theta)} \frac{Q_{bin}}{E_2} \right)^{1/2} \right] \right\}. \quad (2)$$

Here $\mu = m_2/m_1$ is the mass ratio between the target and projectile atoms. Hence the measured kinetic energy of the backscattered projectile is

$$E_k = E_2 \times \frac{(\cos\theta + \sqrt{\mu^2-\sin^2\theta})^2}{(1+\mu)^2} - \Delta E_{bin} - Q_3$$
$$= E_2 f(\theta) - \Delta E_{bin} - Q_3. \quad (3)$$

Since the kinetic energy of a projectile particle after a pure elastic scattering, $E_{elastic}$, is given by

$$E_{elastic} = E_p \times \frac{(\cos\theta + \sqrt{\mu^2-\sin^2\theta})^2}{(1+\mu)^2} = E_p \, f(\theta), \quad (4)$$

the measured inelastic energy loss of Ne, ΔE, is

$$\Delta E = E_{elastic} - E_k = E_p \, f(\theta) - E_k = Q_1 f(\theta) + \Delta E_{bin} + Q_3. \quad (5)$$

We fit this expression to the experimentally measured ΔE-θ curve to extract c and Q_{bin}. It is important to point out that the Ne-2p electron excitation will occur only if the internuclear distance reaches a critical value R_c.

We mention that a similar fitting procedure using a friction force γv^n for the continuous electronic stopping was adopted by Li and MacDonald to analyze their E_p-dependent energy loss of Ne$^+$ scattered off Cu, Ni, and Fe surfaces at two particular θ [32,33]. It regards the interactions as important only within a certain distance H from the topmost atomic layer, where the electron density is close to the bulk value and assumes the trajectory length to be $L_1 = H/\sin\alpha$ and $L_3 = H/\sin(\theta - \alpha)$. This friction force model fails to correctly predict the dependence of the inelastic energy loss on incidence and scattering angles. We chose to use Oen and Robinson's expression because it has been used successfully in previous studies, and because Li and MacDonald [32] have shown that other models like those of Firsov [46] or Kishinevsky and Parilis [45] are not adequate for describing ion scattering from surfaces.
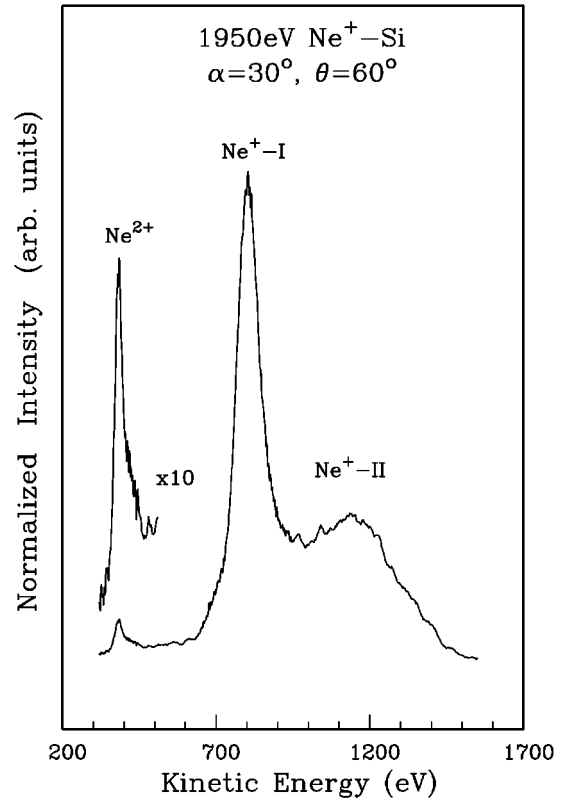
FIG. 1. Energy spectrum for 1950-eV Ne$^+$ scattering from a Si surface at an incidence angle of 30° and scattering angle of 60°. Ne$^+$-I and Ne$^+$-II are due to single and double scattering of Ne$^+$, respectively, and the small feature at about half the energy of Ne$^+$-I is due to a similar single-scattering process leading to reflected Ne^{2+}.

Finally, we point out that an experimental uncertainty $\delta\theta$ in the scattering angle would imply an error in determining E_k. For a fixed E_p and $Q=0$, differentiation of Eq. (3) yields

$$\delta E_k = 2 \left| E_p \frac{\sin\theta}{\sqrt{\mu^2-\sin^2\theta}} \right| \delta\theta, \quad (6)$$

which is a nonmonotonic function of θ. We note that inclusion of inelastic energy loss Q does not modify the results sensitively if $Q \ll E_p$. In our experiments, $\delta\theta = 0.3°$ gives rise to an estimated error of 3.7, 3, and 1.3 eV per 1 keV of primary energy at $\theta = 45°$, 70°, and 100°, respectively, slightly larger than the scatters in our ΔE data (see Figs. 4 and 11). In addition, broadening due to a limited analyzer acceptance angle is also a function of both θ and E_p, and can be evaluated with the same Eq. (6), where δE_k is now interpreted as the instrumental broadening $\Gamma_{instrum}$ and $\delta\theta$ is considered as the acceptance angle. As we will discuss in Sec. III, this broadening is not negligible, and is therefore subtracted from the data to determine the true peak width.

III. RESULTS AND DISCUSSIONS

In Fig. 1 we present a representative as-recorded back-scattered Ne ion spectrum for 1950-eV Ne$^+$ incident on a Si surface for $\alpha = 30°$ and $\theta = 60°$. Besides a pronounced structure at low kinetic energies due to secondary ion emission
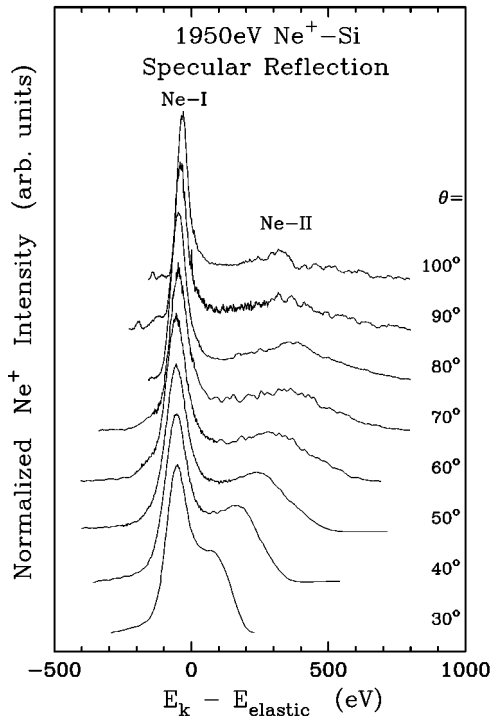
FIG. 2. Backscattered Ne$^+$ spectra for 1950-eV Ne$^+$ incident on a Si surface for some representative scattering angles. The spectra were taken in a specular reflection geometry, and have been corrected for the analyzer transmission factor, background subtracted, and normalized to the same height. The energy scale is referred to the values predicted for elastic Ne-Si single scatterings. Peaks labeled Ne-I and Ne-II are due to single and double scattering, respectively.

(not shown), a large peak can be seen at an energy close to that predicted for a single binary Ne-Si elastic collision together with a structure at higher energies attributed to double scattering. A small peak of backscattered Ne^{2+} was also detected but no structure attributable to the Si$^+$ direct recoil was observed in our experiments.

In the following we will consider separately the inelastic energy loss associated with the singly charged and doubly charged Ne ions backscattered from a Si surface. We will use the data-analysis procedure described above to determine the electronic transition channels involved in the binary collisions, compare with the results of charge fraction, autoionization electron emission, and ion-scattering measurements for this and other similar systems, and propose a description which is consistent with all the experimental results available in the literature.

A. Singly charged Ne$^+$ ions

In Fig. 2 we show a series of Ne$^+$ spectra taken at an incidence energy of $E_p=1950$ eV for various scattering angles, and in Fig. 3 some spectra for fixed $\theta=50°$ and $80°$ and different incident energies. These spectra have been corrected for the analyzer transmission factor, background subtracted, and normalized to the same height. The energy scale refers to the predicted values for elastic Ne-Si binary collisions, E_k-E_{elastic}. It can be noted that the peak labeled Ne-I is shifted due to inelastic energy losses, while the energy
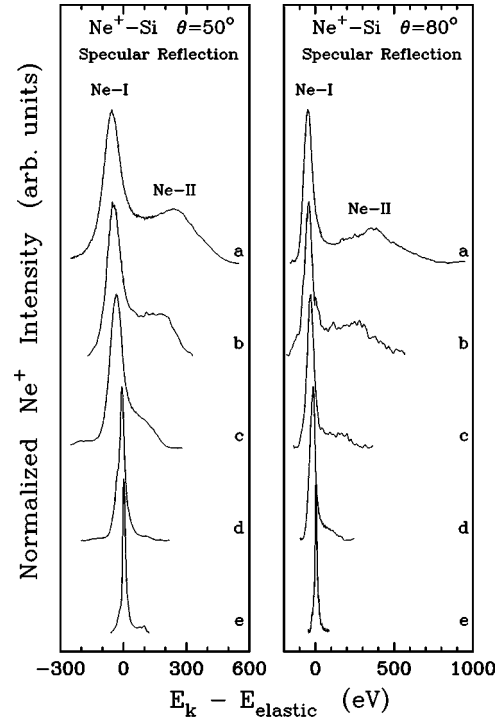
FIG. 3. Ne$^+$ spectra as in Fig. 2, but for two fixed scattering angles and varying primary energies: 1950 eV (curves a), 1400 eV (curves b), 1000 eV (curves c), 700 eV (curves d), and 500 eV (curves e).

position of Ne-II, as well as its spectral shape and relative weight change with θ. Measurements at a fixed θ and varying α (not shown) indicate that for incidence angles larger than 20°, the Ne-I peak can be considered as due to single scattering, while Ne-II is attributed to double scattering.
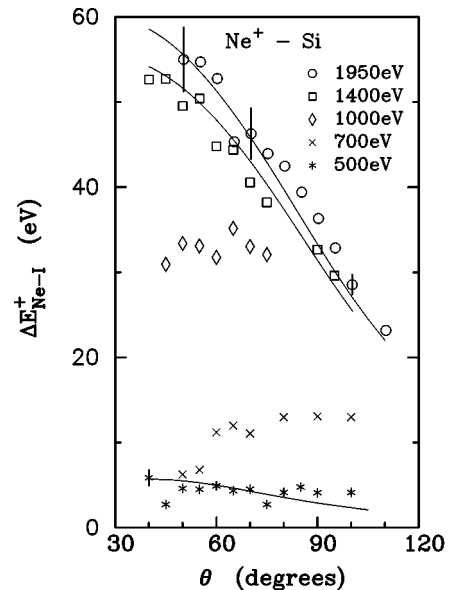
FIG. 4. The inelastic energy loss $\Delta E_{\text{Ne-I}}^+$ suffered by singly scattered Ne$^+$ ions as a function of scattering angle θ for various E_p. $\Delta E_{\text{Ne-I}}^+$ is the difference between the kinetic energy predicted for a binary Ne-Si collision and the experimental value. The continuous curves are the fits for $E_p=1950$ eV (top), 1400 eV (middle), and 500 eV (bottom) described in the text.
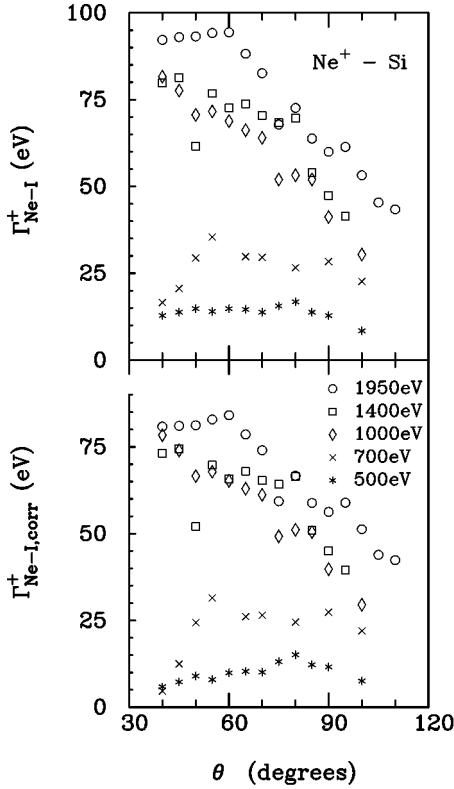
FIG. 5. Upper panel: measured peak width Γ^+_{Ne-I} of the singly scattered Ne$^+$ vs scattering angle θ for various E_p. This is twice the semi-width at half maximum at the low-energy side of the peak. Lower panel: corrected peak width $\Gamma^+_{Ne-I,corr}$ of singly scattered Ne$^+$ calculated as $\Gamma^+_{corr} = [(\Gamma^+_{Ne-I})^2 - (\Gamma_{instrum})^2]^{1/2}$.

The inelastic energy loss $\Delta E^+_{Ne-I} = E_{elastic} - E^+_k$, the full width at half maximum Γ^+_{Ne-I}, and the intensity I^+_{Ne-I} of the Ne-I peak and the total Ne$^+$ intensity I^+_{total} are plotted in Figs. 4–6 as a function of scattering angle θ for five series of data with different incidence energies. Here, the superindex $^+$ denotes the singly charged Ne. Γ^+_{Ne-I} (I^+_{Ne-I}) was obtained by doubling the semiwidth at half maximum (semipeak area) at the low-energy side of the Ne-I peak. The corrected peak widths, $\Gamma^+_{Ne-I,corr} = [(\Gamma^+_{Ne-I})^2 - (\Gamma_{instrum})^2]^{1/2}$, are shown in the lower panel of Fig. 5. All the intensities reported here have been normalized to the beam current.

Figure 4 shows the very different behavior of ΔE^+_{Ne-I} for different incidence energies. For $E_p = 500$ eV, the inelastic energy loss remains nearly constant in the scattering angle range studied, while for $E_p = 700$ eV a slight increase can be noticed. For $E_p = 1400$ and 1950 eV, ΔE^+_{Ne-I} decreases sharply as θ increases. These behaviors indicate quite different inelastic energy-loss mechanisms involved in the collisions.

For $E_p = 500$ eV, the energy loss of about 5–6 eV is too small compared to the first ionization energy of Ne (21.56 eV for an isolated atom which may be reduced if the electron is transferred to the solid). It is also much smaller than the energy required to excite Ne$^+$ $2p^5$ to Ne$^+$* $2p^4 3s$ (27.27 eV) or to excite the ground state Ne ($2p^6$) to $2p^5 3l$ (≥ 16.67 eV). We also notice that even by converting these inelastic losses into the total inelasticity through Eq. (5) the obtained Q_{bin} is still much smaller than
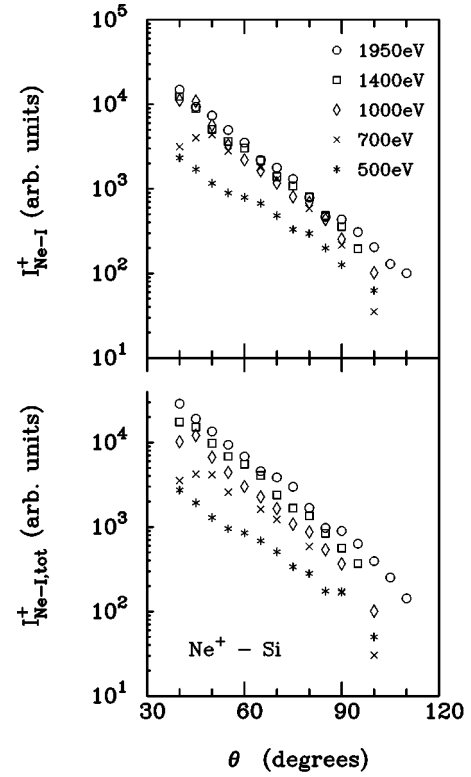
FIG. 6. Intensity of singly scattered (upper panel) and total (lower panel) Ne$^+$ as a function of scattering angle θ for various E_p. They have been normalized to the beam current.

the energies needed for discrete electronic transitions. Therefore, we conclude that in this case the backscattered Ne$^+$ are ions having survived neutralization in both incoming and outgoing trajectories, and that the small inelastic energy loss is due to the excitation of Si valence-band electrons. We fitted the data of ΔE^+_{Ne-I} for $E_p = 500$ eV to Eq. (5) by assuming $Q^+_{bin} = 0$ and $c_1 = c_3 = c^+$, the coefficient for charged Ne$^+$ moving close to the Si surface. The best fit yields $c^+ = 0.68$, and the results are plotted in Fig. 4 as the lowest continuous curve.

As the binary collision becomes more violent, an increase in ΔE^+_{Ne-I} is observed, indicating the occurrence of an additional inelastic loss in the hard collision due to an electronic transition. We fitted the data for $E_p = 1400$ and 1950 eV to Eq. (5) by assuming $Q_{bin} = Q^+_o = \text{const}$. Here c_1 and c_3 were allowed to assume values for Ne$^+$, Ne^0, or Ne^{2+} ($c^0 < c^+ < c^{2+}$). The best fit is for $c_1 = c_3 = c^0 = 0.45$ and $Q_o = 45 \pm 4$ eV, indicating that before and after the binary collision the Ne is most probably in the neutral state. The χ^2 values are relatively large for all other sets, with c^+ or c^{2+} in either incoming or outgoing paths. The fitted ΔE^+_{Ne-I} curves are plotted in Fig. 4 for $E_p = 1400$ and 1950 eV. To better illustrate the discrete inelasticity associated with the electron excitation, we subtracted the contribution due to continuous electronic stopping Q_1 and Q_3 from ΔE^+_{Ne-I} through Eq. (5) and plotted Q^+_{bin} [Eq. (3)] in Fig. 7 versus R_{min}. The dashed lines mark the errors of Q^+_o. For intermediate R_{min}, we used $c_1 = c^0$ and $c_3 = c^0$ for 0.47 Å $\leq R_{min} \leq$ 0.53 Å and $c_3 = c^+$ for 0.53 Å $\leq R_{min} \leq$ 0.59 Å.
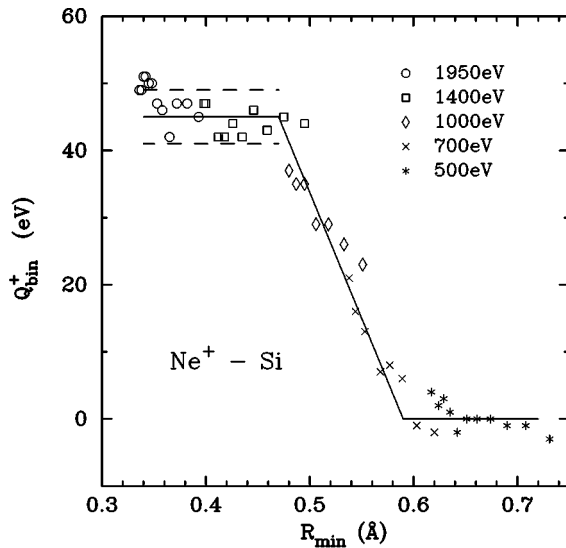
FIG. 7. Inelasticity in the binary collision Q_{bin}^+ for detected Ne$^+$ as a function of distance of closest approach. They are obtained by subtracting the continuous inelastic energy loss of Ne$^+$ from $\Delta E_{Ne\text{-}I}^+$ and converted through Eq. (3). The solid line corresponds to the best fit, and the dashed lines mark the errors of Q_o.

FIG. 8. Qualitative Ne-Si molecular orbital correlation diagram constructed following Ref. [36].

Our results exclude reionization (one electron excitation) of neutralized Ne as the main origin for producing Ne$^+$ in this R_{min} range. $Q_o^+ = 45$ eV agrees well with the energy required to excite two $2p$ electrons from the neutralized Ne into the $2p^4(^1D)3s^2$ autoionization state (45.15 eV, Ref. [47]) and this assignment is consistent with the charge-state indication of c_1 and c_3. Intense electron emission due to the decay of this autoionization state has been observed during Ne$^+$ impact on Si surfaces, and also on Al, Mg, and Na [12,14,15,37,41,48,49].

Our assignment of the energy loss to the double-electron excitation of a neutral Ne is consistent with the experimental evidence that most incoming Ne$^+$ ions are neutralized to the ground state before undergoing a hard collision. Souda *et al.* [38,42] recently reported that backscattered Ne$^+$ has the same line shape and intensity for both neutral and charged projectiles incident on Si, Al, and Mg surfaces, Zampieri, Meier, and Baragiola [37] showed that the Ne $2p^43s^2$ auto-ionization electron spectra are identical for Ne$^+$ and Ne^0 impact on Al, whereas Guillemot *et al.* [14,15] observed that the charge fraction of reflected Ne$^+$ from Si, Al, and Mg surfaces is independent of the projectile charge state.

The inelasticity $Q_o^+ = 45$ eV is also close to the energy for the excitation of two $2p$ electron from Ne $2p^6$ to Ne^{+*} $2p^4(^1D)3s$ (minimal excitation energy 47.35 eV, Ref. [47]). These Ne^{+*} may be finally detected as Ne$^+$ directly or by resonantly capturing an electron from the solid to form Ne** that later autoionizes. According to our model this requires $c_3 = c^+$. Increasing c_3 would result in a reduction of Q_o^+ by a few eV and a worse overall fitting quality. The closer fit and energy match with the excitation of $2p^4(^1D)3s^2$ lead us to favor this assignment, at least for $R_{min} \gtrsim 0.35$ Å. For smaller R_{min}, where the obtained Q_{bin}^+ values are larger, we suggest that one of the excited electrons may indeed be transferred to the solid, resulting in the production of Ne^{+*}. However, the eventually created Ne^{+*} will unlikely survive
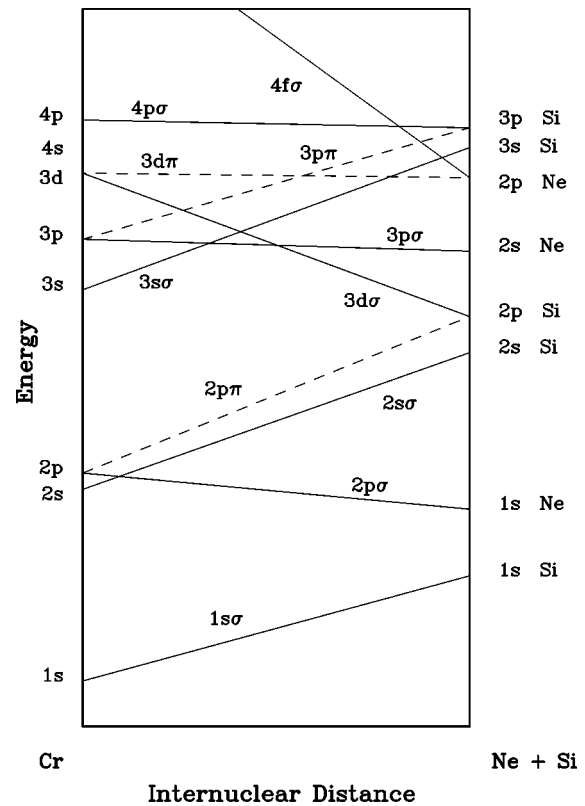
as such when it leaves the surface for the same reason that projectile ions mostly convert to neutrals in the incoming path.

According to the Fano-Lichten-Barat model [35,36], excitation can occur by electron promotion in the transiently formed molecule during the close collision of two atoms as the atomic orbitals (AO's) merge into molecular orbitals (MO's). In Fig. 8 we show a qualitative Ne-Si MO correlation diagram constructed following Ref. [36]. This model predicts the promotion of the $4f\sigma$ MO, correlated to the Ne $2p$ AO, if the minimal internuclear distance reaches a critical value. Radial couplings at curve crossings with high-lying empty levels then can result in Ne $2p$ electron excitation when the two atoms separate [36].

The simultaneous excitation of two electrons in the $4f\sigma$ MO produces a $2p^4(^1D)$ singlet core configuration. As discussed previously [50], close to the excitation site this singlet state can be converted into the ^3P state via an Auger core rearrangement mechanism in which one target valence electron drops into the $4f\sigma$ hole, and an electron with opposite spin in the $3d\pi$ orbital (also correlated to Ne $2p$) is simultaneously excited. This mechanism can be very efficient (up to 80–90 %) resulting in a large $2p^4(^3P)3s^2$ autoionization peak observed for low-energy Ne$^+$ impact on Na, Mg, Al, and Si surfaces [5,49]. These Ne** atoms have a very long lifetime (10^{-13} s, Ref. [51]), so they will decay, on the average, far away from the surface where reneutralization is unlikely. Autoionization produces characteristic electron spectra and results in a singly charged Ne$^+$ final state. Due to the large threshold distance for the two Ne $2p$ electron excitation, large charge fractions of up to 30% for the reflected

Ne were observed for 3 keV scattering from Si surfaces [14], 40% for Al [15], and even as high as 70% for Mg targets [12].

In contrast with our arguments, Souda *et al.* interpreted the same Ne^+ line shape and intensity observed in their ISS with both neutral and charged projectiles at 2 keV as due to reionization of neutralized Ne projectiles by a single $2p$ electron excitation in a hard collision [38,42]. These authors attributed the autoionization electron emission to decay of Ne** formed in two consecutive one-electron excitation events. This interpretation relies on the basic assumption that both the reionization probability and the survival probability of those ions leaving the surface are close to unity. This latter hypothesis is in evident contradiction with the fact that most incoming Ne^+ ions must be neutralized to the ground state, another condition essential for the reionization model.

Our Ne^+-ion spectra show that for 0.59 Å $\geqslant R_{min} \geqslant$ 0.47 Å, the Ne-I peak broadens significantly (see, e.g., Fig. 5 for $E_p=700$ eV) suggesting that both one- and two-electron excitations may occur in this range of R_{min} with a relative probability which increases in favor of the two-electron process as R_{min} decreases. These results are very similar to those for gas-phase Na^+-Ne collisions where the elastic scattering cross section drops dramatically at $R_{min}=1.7$ Å, signaling the opening of inelastic channels [47]. Single-electron excitation is the main process only in a narrow range of 1.39 Å $< R_{min} <$ 1.63 Å, while for smaller internuclear distances double excitation predominates. A smaller critical distance is expected for Ne-Si due to the smaller $2p$ orbital radius of Si.

The identification of the main electronic transition involved in the hard collision leading to the detected Ne^+ also indicates the main final location of the excited Ne $2p$ electrons. It has often been thought that due to the strong coupling of the outer atomic orbitals to the solid valence band, the $2p$ electrons should be transferred irreversibly to the conduction band of the solid and the Ne projectile should exit from the binary collision as an ion [38,39,42]. In this picture, the autoionization states are formed via resonant charge capture in the outgoing trajectory [41]. Our results for low-energy Ne impact on a Si surface show that the excited electrons can be located in the bound 3s atomic outer shells and not lost in the violent collision. Since $4p\sigma$ is the lowest and the first MO that the promoted $4f\sigma$ MO crosses, it is likely that their direct radial coupling would result in a preferential electron transfer into $4p\sigma$, which is correlated to the Ne 3s AO. The upward shift of the 3s level in Ne $2p^4(^1D)3s^2$ due to image charge interactions is not sufficient to cause a resonant electron tunneling to the solid (atomic binding energy BE is equal to 7 eV; see Ref. [48]). Results of Fig. 7 also suggest that the probability of transferring the excited electron to the solid may increase as the internuclear distance between the colliding atoms further reduces.

Figure 6 shows that for a given scattering geometry the intensity of backscattered Ne^+ increases with increasing primary energy, while for a fixed E_p it decreases sharply with scattering angle. These behaviors depend on many factors such as the scattering cross section, surface shadowing and blocking, excitation and neutralization probability, the ion penetration probability, double and multiple scattering, etc.

The large width associated with the Ne-I peak (Fig. 5) can originate from different contributions. Quasisingle scattering

(QSS), i.e., a slight deviation from the original trajectory, can result in a smaller effective scattering angle in the binary collision, and thus a smaller elastic energy transfer to the target Si atom. Scattering from the subsurface layers, on the other side, is responsible for the broadening at the low energy side. For large R_{min} (see the series of $E_p=500$ eV), the detected Ne^+ are those projectile ions that have survived Auger neutralization in both incoming and outgoing paths and contributions from QSS and subsurface scattering must be very small since they both will strongly reduce the ion survival probability. Conversely, for $R_{min}<0.47$ Å, these contributions can be substantial given that the projectile is in a neutral state both before and after the hard collision. Trajectory length distribution, charge exchange and excitation of electron-hole pair in the solid are other sources of energy straggling. Further, the distribution of final excitation states can also contribute to the peak broadening.

Regarding the role of double-scattering (DS) events, though a clear identification of the transition channel(s) is quite difficult in the present experiment as the Si surface was amorphized, some considerations can still be made from our single-scattering results. For primary energies in the keV range, the small cross section for one-electron excitation in SS makes unlikely the formation of Ne** in two consecutive collisions. The large probability of Auger neutralization should also result in a negligible creation of Ne^+ in DS. We suggest that the simultaneous excitation of two electrons in one of the two encounters may also be the main mechanism
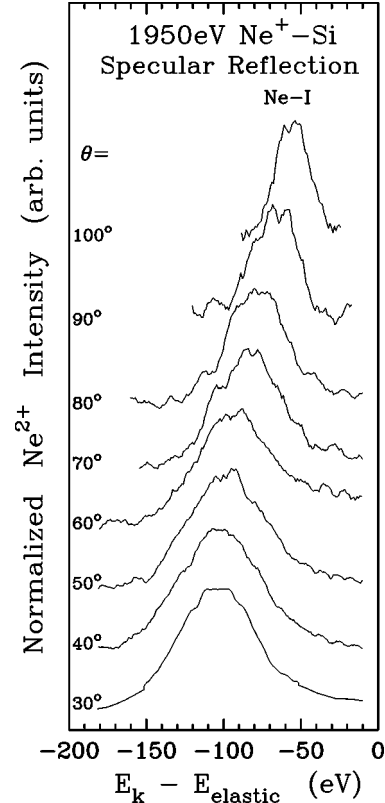
FIG. 9. Ne^{2+} spectra corrected for the analyzer transmission factor, background subtracted, and normalized for $E_p=1950$ eV and various scattering angles. These doubly charged ions were detected at half of their kinetic energies, and the energy scale refers to the values predicted for single elastic scatterings.
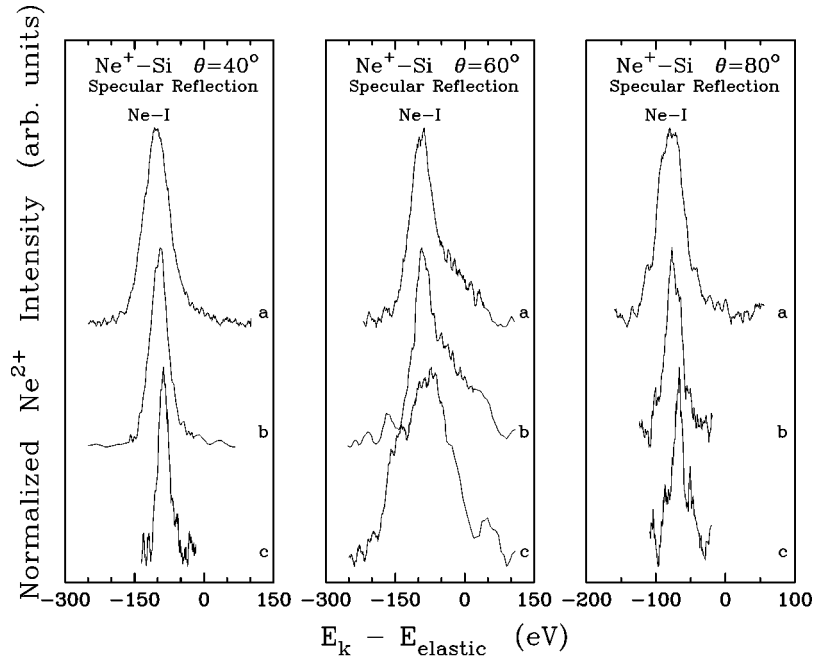
FIG. 10. Ne^{2+} energy spectra as in Fig. 9, but for three fixed scattering angles and E_p=1950 eV (curves a), E_p=1400 eV (curves b), and E_p=1000 eV (curves c).

in DS. More detailed studies on this subject are currently underway, and will be discussed elsewhere [52].

B. Doubly charged Ne^{2+} ions

In Figs. 9 and 10 are displayed some representative Ne^{2+} spectra for E_p=1950 eV and varying θ, and for three fixed θ= 40°, 60°, and 80° and different E_p. These spectra have been corrected for the analyzer transmission factor, background subtracted, and normalized to the same height. They have a nearly symmetric Gaussian line shape, and the large structure due to double scattering is absent. It is important to note that, in our experimental conditions, Ne^{2+} ions are detected only for $R_{\min} \lesssim 0.59$ Å (E_p=1000 eV and θ=38°) indicating the existence of a threshold distance.

Results of our data analysis on these Ne^{2+} spectra are presented in Figs. 11–13 for the inelastic energy loss $\Delta E_{\text{Ne-I}}^{2+}$, the width $\Gamma_{\text{Ne-I}}^{2+}$, and the intensity $I_{\text{Ne-I}}^{2+}$ of the Ne-I peak, which coincides with the total intensity I_{total}^{2+}, as a function of scattering angle θ. The corrected width $\Gamma_{\text{Ne-I,corr}}^{2+}$ is shown in the lower panel of Fig. 12. To identify the main electronic transition leading to Ne^{2+}, we fitted $\Delta E_{\text{Ne-I}}^{2+}$ using the procedure described in Sec. II B. Our fitting yields $c_1 = c^+ = 0.68$, $c_3 = c^{2+} = 0.74$, and $Q_o^{2+} = 86 \pm 5$ eV. The results are shown in Fig. 11 as continuous curves. In Fig. 14 we show Q_{bin}^{2+} versus $R_{\min}$ after subtracting the continuous inelastic loss from $\Delta E_{\text{Ne-I}}^{2+}$ and converting it through Eq. (2).

We notice that $Q_o^{2+} = 86$ eV is too small compared to the energy needed to excite a Si $2p$ electron (98.3 eV, Ref. [53]), and also too far from the ionization energy of Ne$^+$ (41.08 eV for an isolated ion) or the energy needed for a double ionization of a neutralized Ne atom or a surviving Ne$^+$ ion (65.8 and 107 eV, respectively, for free atoms). Inspection of the energy levels suggests that this inelasticity can be attributed to transitions involving a double Ne $2p$ electron excitation

from Ne$^+$ $2p^5$ to Ne^{2+}* $2p^3(^2D, \, ^2P)3s$ (84.9 and 87.5 eV, Ref. [54]). This assignment is consistent with the charge-state indication of the fitting parameters c_1 and c_3.

Ne^{2+}* can be formed from a surviving Ne$^+$ via a simultaneous two electron excitation in the $4f\sigma$ MO, provided that the original $2p$ vacancy is located in the correlated $3d\pi$ MO. When these Ne^{2+}* leave the surface, they can undergo an Auger deexcitation or radiative decay into Ne^{2+}. Alternatively, they may capture one electron from the solid
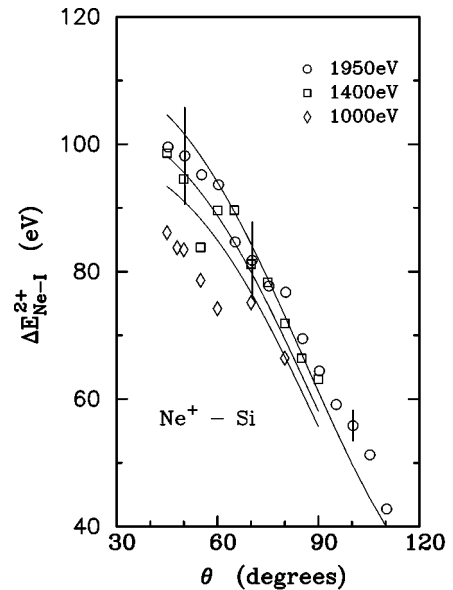
FIG. 11. Inelastic energy loss $\Delta E_{\text{Ne-I}}^{2+}$ suffered by singly scattered Ne^{2+} ion as a function of scattering angle θ for various E_p. The continuous curves are the fits described in the text for E_p=1950 eV (top), 1400 eV (middle), and 1000 eV (bottom).
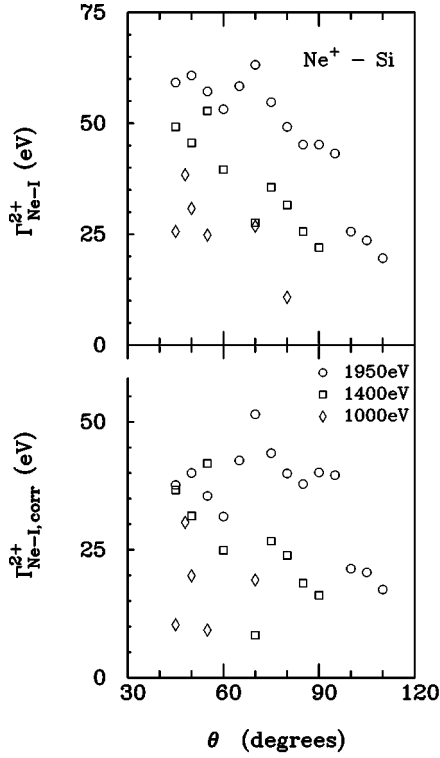
FIG. 12. Measured full width at half maximum $\Gamma^{2+}_{\text{Ne-I}}$ (upper panel) and the corrected peak width $\Gamma^{2+}_{\text{Ne-I,corr}}$ (lower panel) of the singly scattered Ne^{2+} peak vs scattering angle θ.

to form Ne^{+**} autoionization states which, owing to their relatively long lifetime ($>5 \times 10^{-14}$ sec; see Ref. [55]), may decay to final Ne^{2+} far from the surface where reneutralization is unlikely. The characteristic autoionization electron emission from Ne^{2+*} has been detected and identified [41,56,57].
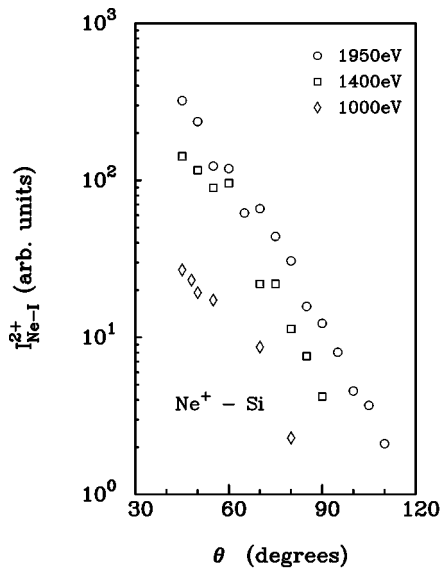
FIG. 13. Intensity of singly scattered Ne^{2+} as a function of scattering angle θ for various E_p. They have been normalized to the beam current. Note that the values coincide with the total Ne^{2+} intensities because the double-scattering peak is absent in the spectra of Figs. 8 and 9.
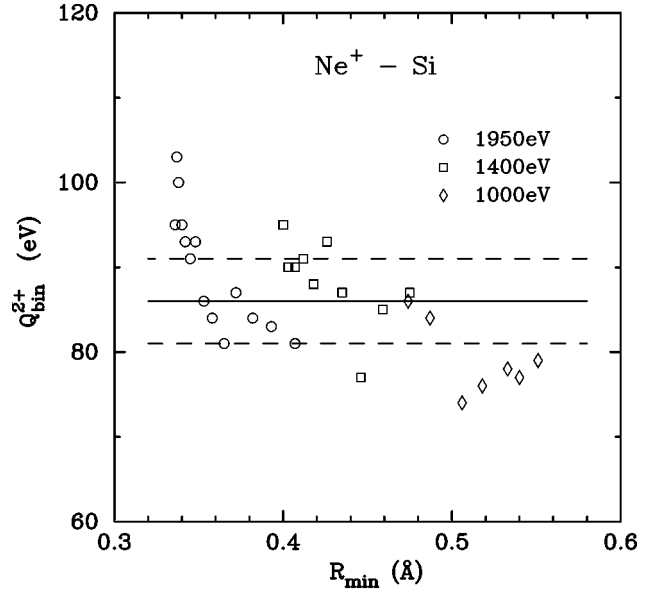
FIG. 14. Inelasticity in the binary collision Q^{2+}_{bin} for detected Ne^{2+} as a function of the distance of closest approach. They are obtained by subtracting the continuous inelastic energy loss of Ne^{2+} from $\Delta E^{2+}_{\text{Ne-I}}$ and converted through Eq. (3). The solid line is $Q^{2+}_o = 86$ eV, and the dashed lines mark the errors.

We note from Fig. 14 that the obtained Q^{2+}_o is somewhat smaller for $R_{\text{min}} \geqslant 0.5$ Å (see also the fit for $E_p = 1000$ eV in Fig. 12). It may be an indication that in this case both excited electrons are located in the bound Ne atomic $3s$ or $3p$ levels (for example, the transition energy is 75 eV for $2p^5 \rightarrow 2p^3(^2D)3s3p$) without being transferred to the solid. A clear distinction between different final states is not straightforward since different proportionality constants c should be used and the results of our data analysis would not be reliable. As we discussed in Sec. III A for Ne^+ (see Fig. 7), the final location of the excited electron may indeed depend on the value of R_{min} reached in the collision, and the probability of transferring one or two electrons to Si is larger for smaller R_{min}.

Comparison with the results for Ne^+ indicates that the same crossings of the promoted $4f\sigma$ MO with high-lying empty levels are involved in both Ne-Si and Ne^+-Si systems. Our recent experiments confirm that the very same inelasticity, and thus the same transition, also occurs in Ne^+-Al [16]. It is important to point out that a fundamental requirement for the creation of a $2p^3$ core in a single collision is that the incoming Ne^+ ion must have survived the Auger neutralization before undergoing a hard collision, and that the initial hole is located in the correlated $3d\pi$ MO. This explains why the Ne^{2+} ions are not detected in single scattering of neutrals [38,42], and why their intensity is very small relative to that of Ne^+ ions.

The intensity ratio $\rho_{\text{Ne-I}} = I^{2+}_{\text{Ne-I}}/I^+_{\text{Ne-I}}$ and $\rho_{\text{total}} = I^{2+}_{\text{total}}/I^+_{\text{total}}$ between the doubly and singly charged Ne ions are plotted in Fig. 15 versus θ. We note that these values are generally smaller than those reported by Souda *et al.* [38], probably because the latter authors did not correct their ion-scattering spectroscopy (ISS) data for the analyzer transmission factor. The values of ρ_{total} found here are in good agreement with those reported by Wittmaack [58]. Interestingly, these values
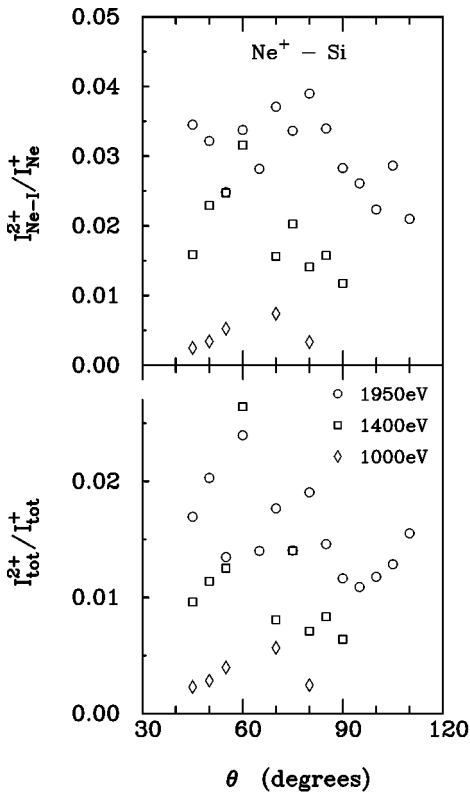
FIG. 15. Intensity ratio between Ne^{2+} and Ne$^+$ as a function of the distance of closest approach in single (upper panel) and total (lower panel) scattering events.

are consistent with the total intensity ratio between the Ne $2p^3 3l3l'$ and $2p^4 3s^2$ autoionization electron lines observed in our previous studies for 1-keV Ne$^+$-Al at $\alpha = 20°$ [41]. This provides additional independent support to our assignment of the Ne^{2+} feature in ISS to a double electron excitation of Ne$^+$.

The observation of the Ne^{2+} single scattering peak only for charged projectiles but not for neutrals incident on Si, Al, and Mg surfaces led Souda *et al.* [38,42] to conclude that Ne^{2+} originates from a one-electron excitation of survived Ne$^+$. This conclusion is inconsistent with our inelastic energy-loss measurements. In fact, our results exclude direct reionization as the main production mechanism not only for detected Ne$^+$ but also for Ne^{2+}.

Recently, Hird, Armstrong, and Gauthier [40] detected backscattered multicharged projectile ions by scattering of Ne$^+$ off a Si surface. In contrast to our interpretation within the framework of molecular orbital curve-crossing model, they argued that these ions should result from a double-electron transfer process in which an electron in the $4f\sigma$ MO drops into $3s\sigma$ (or $3d\pi$) MO, and simultaneously another electron from deeper $3d\sigma$ is excited to $3s\sigma$ (or $3d\pi$). A subsequent Auger transition would then fill the $3d\sigma$ hole to produce a multicharged ion. This model, originally developed to interpret the inelastic loss in gas phase C$^+$-Ne and N$^+$-Ne collisions [59,60] at large internuclear distances, cannot be applied here, since neither the $3s\sigma$ MO (correlated to Si $3s$) nor the $3d\pi$ MO (correlated to Ne $2p$) has two holes to accommodate the eventually transferred electrons. Moreover, as suggested by Barat and co-workers [59,60], once the internuclear distance reaches that for the curve crossings,

electron transfer between the crossing states should be far more important than other electron transfer mechanisms. The similar threshold distance of 0.59 Å observed for double-electron excitation in both Ne$^+$-Si and Ne^0-Si found in our study, which agrees reasonably well with the value of 0.56 Å reported in Ref. [40] for observation of Ne^{2+}, provides further argument against the double electron transfer mechanism. We also suggest that triply ionized Ne^{3+} observed in Ref. [40] may result from the very same two $4f\sigma$ electron excitation of survived Ne$^+$ with both excited electrons transferred to the solid. Indeed, the threshold distance was reported to be 0.164 Å, far below the $R_{\min}$ values studied here, and the large projectile velocity would assure that a portion of the incoming Ne$^+$ and outgoing Ne^{3+} survives neutralization.

The relatively small and nearly constant linewidth of the SS peak of Ne^{2+} (see the lower panel of Fig. 12) indicates that contributions from quasisingle scattering and subsurface scattering are quite small relative to the case of Ne$^+$. This is expected since the Ne projectile is now in a charged state in both incoming and outgoing path, and its survival probability will be greatly reduced if its trajectory length is increased. We note that the average value of about 30 eV for Ne^{2+} is larger than that of 10 eV for surviving Ne$^+$ ions (see data of $E_p = 500$ eV of Fig. 5). This additional broadening may be partly due to factors related to the final-state distribution in the excitation and charge exchange for forming Ne^{+**} autoionization states.

The absence of double and multiple scattering in Ne^{2+} confirms that these ions originate only from scattering of Ne$^+$ off the topmost layer. We mention that a pronounced double-scattering feature, however, is clearly observed for Ne^{2+} for the Ne$^+$-Al system [42,16]. A detailed discussion on the mechanism involved in these DS events will be presented elsewhere [52].

IV. CONCLUSIONS

In conclusion, we presented a detailed energy-loss study on singly and doubly charged Ne ions backscattered from a Si surface. The main results can be summarized as follows:

(1) Singly backscattered Ne$^+$ and Ne^{2+} ions originate mainly from the same double $2p$ electron excitation mechanism via $4f\sigma$ molecular orbital curve crossings. Most incoming Ne$^+$ are neutralized to the ground state, and electron excitation in the binary collision results in the formation of Ne**, while a few survived Ne$^+$ ions with an initial hole located in $3d\pi$ can be excited to form Ne^{2+*}. Autoionization decay in vacuum far away from the surface where reneutralization is unlikely, or direct decay of excited ions, produces final scattered Ne$^+$ and Ne^{2+}.

(2) For low-energy collisions, the excited $2p$ electrons are most probably located in the atomic Ne $3l$ outer orbitals, presumably due to the crossing of the promoted $4f\sigma$ MO with the $4p\sigma$ MO prior to crossings with other high-lying empty levels. As the internuclear distance becomes smaller, one or two excited electrons may be transferred to the solid.

(3) The threshold internuclear distance for Ne $2p$ electron excitation is found to be 0.59 Å for both Ne^0 and Ne$^+$. The relative weight of single-electron excitation for Ne^0 decreases with decreasing $R_{\min}$, and becomes very small

with respect to the double excitation for $R_{min} \leq 0.47$ Å.

(4) Quasisingle scattering and subsurface scattering contribute greatly to the broadening of the Ne^+ signal, but not to that of Ne^{2+}. A pronounced double-scattering peak is seen in the singly charged ion spectra but is absent for the doubly charged one.

[1] R. S. Williams, in *Low Energy Ion-Surface Interactions*, edited by J. W. Rabalais (Wiley, Chichester, 1994), p. 1.

[2] P. G. Bertrand and J. W. Rabalais, in *Low Energy Ion-Surface Interactions* (Ref. [1]), p. 55.

[3] E. W. Thomas, Vacuum **34**, 1031 (1984).

[4] S. Valeri, Surf. Sci. Rep. **17**, 85 (1993).

[5] F. Xu, Mod. Phys. Lett. B **9**, 319 (1995).

[6] H. D. Hagstrum, in *Inelastic Ion- Surface Collisions*, edited by N. H. Tolk, J. C. Tully, W. Heiland, and C. W. White (Academic, New York, 1977).

[7] W. Heiland and E. Taglauer, in *Inelastic Ion-Surface Collisions* (Ref. [6]).

[8] H. D. Hagstrum, Phys. Rev. **96**, 325 (1954); **96**, 336 (1954).

[9] H. D. Hagstrum, Phys. Rev. **104**, 672 (1956).

[10] H. Shao, D. C. Langreth, and P. Nordlander, in *Low Energy Ion-Surface Interactions* (Ref. [1]) p. 117.

[11] J. W. Rabalais, J. N. Chen, and R. Kumar, Phys. Rev. Lett. **55**, 1124 (1985).

[12] O. Grizzi, M. Shi, H. Bu, J. W. Rabalais, and R. A. Baragiola, Phys. Rev. B **41**, 4789 (1990).

[13] K. A. H. German, C. B. Weare, and J. A. Yarmoff, Phys. Rev. Lett. **72**, 3899 (1994).

[14] L. Guillemot, S. Lacombe, M. Maazouz, E. Sanchez, and V. A. Esaulov, Surf. Sci. **356**, 92 (1996).

[15] L. Guillemot, S. Lacombe, V. N. Tuan, V. A. Esaulov, E. Sanchez, Y. A. Bandurin, A. I. Dashchenco, and V. G. Drobnich, Surf. Sci. **365**, 353 (1996).

[16] F. Ascione, G. Manicò, P. Alfano, A. Bonanno, N. Mandarino, A. Oliva, and F. Xu, Nucl. Instrum. Methods Phys. Res. Sec. B (to be published).

[17] G. Manicò, F. Ascione, N. Mandarino, A. Bonanno, P. Riccardi, P. Alfano, P. Zoccali, A. Oliva, M. Camarca, and F. Xu, Surf. Sci. Lett. (to be published).

[18] L. K. Verhey, B. Poesema, and A. L. Boers, Nucl. Instrum. Methods **132**, 565 (1976).

[19] T. M. Buck, G. H. Wheatley, and L. K. Verheij, Surf. Sci. **90**, 635 (1979).

[20] S. B. Luitjens, A. J. Algera, E. P. Th. M. Suurmeijer, and A. L. Boers, Surf. Sci. **99**, 631 (1980).

[21] R. Kumar, M. H. Mintz, and J. W. Rabalais, Surf. Sci. **147**, 15 (1984).

[22] T. M. Thomas, H. Neumann, A. W. Czanderna, and J. R. Pitts, Surf. Sci. **175**, L737 (1986).

[23] R. Souda and M. Aono, Nucl. Instrum. Methods Phys. Res. B **15**, 114 (1986).

[24] R. Souda, T. Aizawa, C. Oshima, S. Otani, and Y. Ishizawa, Surf. Sci. **194**, L119 (1988).

[25] R. Souda, T. Aizawa, C. Oshima, and Y. Ishizawa, Nucl. Instrum. Methods Phys. Res. B **45**, 364 (1990).

[26] S. Tsuneyuki and M. Tsukada, Phys. Rev. B **34**, 5758 (1986).

[27] Y. Muda and D. M. Newns, Phys. Rev. B **37**, 7048 (1988).

[28] F. Shoji, Y. Nakayama, K. Oura, and T. Hanawa, Nucl. Instrum. Methods Phys. Res. B **33**, 420 (1988).

[29] W. Heiland and E. Taglauer, Nucl. Instrum. Methods Phys. Res. **132**, 535 (1976).

[30] W. Heiland, H. G. Schaffler, and E. Taglauer, Surf. Sci. **35**, 381 (1979).

[31] T. M. Buck, W. E. Wallace, R. A. Baragiola, G. H. Wheatley, J. B. Rothman, R. J. Gorte, and J. G. Tittensor, Phys. Rev. B **48**, 774 (1993).

[32] T. Li and R. J. MacDonald, Phys. Rev. B **51**, 17 876 (1995).

[33] T. Li and R. J. MacDonald, Surf. Sci. **351**, 319 (1996).

[34] K. A. H. German, C. B. Weare, and J. A. Yarmoff, Phys. Rev. B **50**, 14 452 (1994).

[35] U. Fano and W. Lichten, Phys. Rev. Lett. **14**, 627 (1965).

[36] M. Barat and W. Lichten, Phys. Rev. A **6**, 211 (1972).

[37] G. Zampieri, F. Meier, and R. Baragiola, Phys. Rev. A **29**, 116 (1984).

[38] R. Souda, K. Yamamoto, W. Hayami, T. Aizawa, and Y. Ishizawa, Phys. Rev. Lett. **75**, 3552 (1995).

[39] Q. B. Lu, R. Souda, D. J. O'Connor, B. V. King, and R. J. MacDonald, Phys. Rev. B **54**, R8389 (1996).

[40] B. Hird, R. A. Armstrong, and P. Gauthier, Phys. Rev. A **49**, 1107 (1994).

[41] F. Xu, N. Mandarino, A. Oliva, P. Zoccali, M. Camarca, A. Bonanno, and R. A. Baragiola, Phys. Rev. A **50**, 4040 (1994).

[42] R. Souda, K. Yamamoto, W. Hayami, T. Aizawa, and Y. Ishizawa, Surf. Sci. **363**, 139 (1996).

[43] O. S. Oen and M. T. Robinson, Nucl. Instrum. Methods Phys. Res. **132**, 647 (1976).

[44] W. Heiland and A. Närmann, Nucl. Instrum. Methods Phys. Res. B **78**, 20 (1993).

[45] L. M. Kishinevsky and E. S. Parilis, Izv. Akad. Nauk SSSR Ser. Fiz. **26**, 1409 (1962); see also E. S. Parilis, L. M. Kishinevsky, N. Yu. Turaev, B. E. Baklitzky, F. F. Umarov, V. Kh. Verleger, S. L. Nizhnaya, and I. S. Bitnesky, *Atomic Collisions on Solid Surfaces* (North-Holland, Amsterdam, 1993), p. 18.

[46] O. B. Firsov, Zh. Eksp. Teor. Fiz. **36**, 1517 (1959) [Sov. Phys. JETP **36**, 1076 (1959)].

[47] J. O. Olsen, T. Andersen, M. Barat, Ch. Courbin-Gaussorgues, V. Sidis, J. Pommier, J. Agusti, N. Andersen, and A. Russek, Phys. Rev. A **19**, 1457 (1979).

[48] G. E. Zampieri and R. A. Baragiola, Surf. Sci. **114**, L15 (1982).

[49] A. Bonanno, P. Zoccali, and F. Xu, Phys. Rev. B **50**, 18 525 (1994).

[50] F. Xu, R. A. Baragiola, A. Bonanno, P. Zoccali, M. Camarca, and A. Oliva, Phys. Rev. Lett. **72**, 4041 (1994).

[51] The lifetime of the Na $2p^5 3s^2$ autoionization state is calcu-

lated to be 2×10^{-13} s; see O. I. Zatsarinny and L. A. Bandurina, J. Phys. B **26**, 3765 (1993). Those of the Ne $2p^4 3s^2$ states are expected to be of the same order.

[52] G. Manicò, F. Ascione, P. Alfano, A. Bonanno, A. Oliva, and F. Xu (unpublished).

[53] W. A. Metz, K. O. Legg, and E. W. Thomas, J. Appl. Phys. **51**, 2888 (1980).

[54] G. N. Ogurtsov, V. M. Mikushkin, I. P. Flaks, A. V. Kuplyauskene, and Z. I. Kuplauskene, Opt. Spectrosk. **54**, 391 (1983) [Opt. Spectrosc. **66**, 299 (1983)].

[55] R. Morgenstern, A. Niehaus, and G. Zimmermann, J. Phys. B **13**, 4811 (1980).

[56] T. E. Gallon and A. P. Nixon, J. Phys.: Condens. Matter **4**, 9761 (1992).

[57] F. Xu and A. Bonanno, Phys. Lett. A **180**, 350 (1993).

[58] K. Wittmaack, Surf. Sci. **345**, 110 (1996).

[59] D. Dowek, J. Krutein, U. Thielmann, J. Fayeton, and M. Barat, J. Phys. B **12**, 2553 (1979).

[60] U. Thielmann, J. Krutein, and M. Barat, J. Phys. B **13**, 4217 (1980).